Fracture and Slow Crack Characteristics of Nuclear Grade Graphite using the Double Torsion Beam Technique

T.H. Becker and R.B. Tait
University of Cape Town, Cape Town, South Africa

1. Introduction

Artificial polycrystalline nuclear grade graphite is used for structural components as well as neutron moderators in nuclear reactors. South Africa is currently developing a Pebble Bed Modular Reactor (PBMR), which is a high temperature helium gas cooled reactor, based on earlier German experiences [1]. The core of this reactor type is composed of many graphite brick like components, which serve as both an inner and outer reflector and a passive heat transfer medium. Internal shrinkage, changes induced by irradiation and thermal stresses generated during operation may lead to crack initiation in the brittle graphite from keyway corners and other discontinuities. The structural integrity of the graphite, best assessed by the fracture mechanics methodology, plays in important role as any damage or cracking could leak heat or radiation to the core barrel and the outer pressure vessel shell, which may result in unsatisfactory consequences.

Although many artificial graphites do not perfectly satisfy the conditions of linear elastic fracture mechanics (LEFM), early fracture mechanics of artificial graphite, such as the nuclear grade graphite, has been conducted on a linear elastic hypothesis by using the critical stress intensity factor K_{Ic} and the critical strain energy release rate G_{Ic} [2][3]. There is some concern, however, as large deviations in results [4] and non linearity has been reported [5]. These are explained by extensive micro cracking and irreversible slip deformation along the basal planes of graphite crystallites [2][6]. Such inelastic micro cracking and plastic slippage cause marked non linearity. Attempts have been made to account for this non linearity in the load-displacement relation of graphite. Sakai et al [5] used an energy principle, where they used chevron notch (CN) compact tensile specimens on isotropic fine grain size polycrystalline graphite, IG-11. They measured the nonlinear elastic-plastic fracture parameters under loading and unloading of the specimen. Their results found that about *38%* of the total fracture energy was consumed as "plastic" energy and concluded that for zero plastic energy dissipation the fracture parameters converge to a lower limit of *73 J/m²*, which equates to a fracture toughness of *0.27 MPa√m*. Similarly, Shi et al [7] attempted a fracture analysis using sandwiched three point bending specimens and determined the fracture toughness as *1.2 MPa√m* for IG-110 nuclear grade graphite. They reported that the test sandwich configuration enabled stable crack growth to occur, allowing for optical imaging to determine accurately the length of the extending crack.

The Double Torsion Beam (DTB) configuration may be used for fracture and slow crack growth characteristics of highly brittle materials. The technique was first introduced by Outwater and Gerry [8] and Kies and Clark [9] in the late

---

1960's. The development of DTB technique for various materials have been addressed in several different investigations such as, Evans [10], William and Evans [11], Outwater and Murphy [12], Mc Kinney and Smith [13], Virkar and Johnson [14], Trantina [15], Fuller [16], Pletka and Fuller [17], amongst others, and the DTB method has been reviewed by Tait et al [18] and Shyam [19]. Corrections to the technique were proposed by Leevers et al [20][21][22], Chevalier et al [23] and Ciccotti et al.[24][25][26][27]. In the last forty years, the double-torsion test has been extensively used in the evaluation of the relation between stress intensity factor, K_I, and crack velocity, V, during sub critical crack growth assuming LEFM conditions. The DTB technique allows for stable controlled crack growth and for relatively large stable crack extensions (up to 75mm for a specimen of 150mm length), unlike sandwiched bending specimens where crack extension is seldom longer than 1-2mm [7]. However, the DTB technique is yet to be standardized, with some concern over the assumption of a constant K regime, and as it stands momentarily, there has been limited application of the technique to linear elastic-plastic fracture mechanics (LEPFM). This paper utilises DTB specimens of nuclear graphite in an attempt to generate useful fracture toughness and crack velocity V vs. stress intensity K characterisation information.

2. The Double Torsion Beam technique

The DTB specimen comprises a rectangular thin plate supported in four point bending at one end. The specimen is considered as two separate halves, which, when loaded, result in a torsional deformation or twist of each half through an angle θ between which the crack propagates. The two specimen halves deform independently around the crack section. A schematic diagram of the DTB specimen is shown in Fig. 1, where: a is the crack length, a_o the notch length, W_m the applied moment arm due to load P with deflection y at the load points. In its simplest form the specimen has dimensions: length L, width W and thickness d.
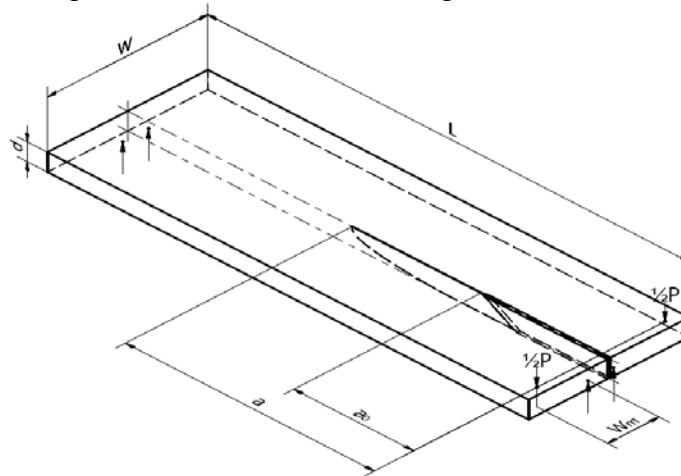

Fig. 1: The Double Torsion Beam (DTB) Specimen.

The DTB has the unique feature of stable crack propagation at constant load, which results in a constant stress intensity plateau over the middle half of the specimen length, as a first approximation. The derivations of the stress intensity K_I, under the assumption of mode I, and crack velocity, take advantage of the linear compliance relationship C, which was experimentally determined as,

$$C(a) \approx \frac{y}{P} = B_E a + D_E \tag{1}$$

where B_E is the slope and D_E is the y intercept.

The compliance relationship, under the assumption of LEFM, with use of the Irwin expression in mode I crack opening, is used to solve for G_c and hence K_c. The expression for K_I is given below under the assumption of plane strain

$$K_I(P) = P \sqrt{\frac{B_E \mu}{d(1-v)\psi(t,W)}} \tag{2}$$

where μ is the shear modulus, v is poisson's ratio and $\psi(t,W)$ a thickness correction factor [16]. B_E is often calculated as the analytical stiffness by $B_E = 3w_m{}^2/Wd^3\mu$. The fracture toughness may be calculated by substituting P with the plateau load or critical load P_c in Eq. (2).

Similarly, the crack velocity may be calculated by the commonly used load relaxation technique to obtain indirectly the sub-critical crack propagation behaviour of brittle materials. According to this technique, a pre-cracked double-torsion test specimen is loaded to below the expected fracture load (*0.90–0.95*P_c*). The crosshead of the testing machine is then held at a fixed position and the increase in compliance of the test specimen from sub-critical crack growth leads to a relaxation of the load with time. The expression is used to determine crack velocities

$$V(P,t) \equiv \frac{da}{dt}\bigg|_y = \phi \frac{-P_{i,f}}{P^2}\left(a_{i,f} + \frac{D_E}{B_E}\right)\left(\frac{dP}{dt}\right)_y \tag{3}$$

where $P_{i,f}$ and $a_{i,f}$ are the initial or final load and crack lengths respectively. ϕ is crack velocity averaging value, as the crack speed varies, due the curved crack front profile, determined by Pollet and Burns [28]. Other techniques for slow crack growth determination using the DTB technique include the constant displacement technique and the constant load technique. Crack velocity-stress intensity (*VK*) data is the plot of K_I vs. V given by Eq. (2) and (3) respectively.

3. Experimental Details

The experimental procedure to determine the fracture toughness and slow crack growth characteristics made use of the DTB technique. A DTB fixture was specifically constructed to ensure straight controlled crack propagation, as un-grooved specimens were used. The loading machine was a Zwick screw driven tensile/compressive testing machine using a 20kN load cell.

3.1. Specimen Details

The graphite used was artificial nuclear grade supplied by PBMR. The graphite has a coarse structure (a grain size of typically *2mm*) and of grade NVG10 and exhibited distinct grain orientations or anisotropy due to the extrusion process of

manufacture. Because of the anisotropy, specimens were machined so that crack propagation was either parallel or perpendicular to the dominant grain direction. Mechanical material properties were supplied by PBMR, where Young's modulus was assumed at *10GPa*, tensile strength of *25MPa*, Poisson's ratio at *0.2* and the shear modulus at *4 GPa*.

The DTB specimen dimensions were length *150mm*, width *50mm* and thickness of *4.15mm*. Each specimen was fitted with a starter notch of length of *20mm* at a *45°* angle. The specimens were sliced from a large block supplied and machined to shape on a CNC milling machine at the University's workshop. Care was taken to minimally stress the material so to avoid any prior damage to the specimens, and also to ensure dimensional reliability.

3.2. Linear Elastic Fracture Mechanics

For comparative purposes, K_{Ic} and G_{Ic} were evaluated for the graphite material. A modified approach was employed, which is a numerical approach of Irwin's relationship, to solve for the toughness. As a constant load plateau is present in the DTB specimen Irwin's relationship may be numerically solved under the assumption of LEFM by

$$G = \frac{1}{2}P^2\frac{dC}{dA} \approx \frac{1}{2d}P^2\frac{(C_2-C_1)}{(a_2-a_1)} \tag{4}$$

where a_1 and a_2 represent the crack length measurements at C_1 and C_2 of the 1st and 2nd unloading-loading curve, respectively. Fig. 2(a) presents a graphical representation of the methodology discussed. Essentially this calculates the area enclosed by the loading and unloading curves and if plotted against crack length becomes similar to Albuquerque's [29] methodology for *R*-curve behaviour for LEFM. The modified technique was in good agreement with the original proposed technique (Eq. (2)) for PMMA specimens tested. This modified technique allows for the exclusion of many proposed corrections for the DTB technique.
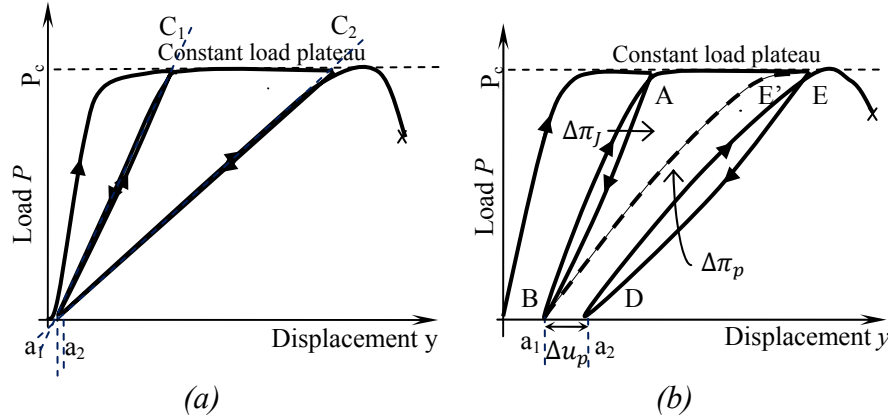

(a)   *(b)*

Fig. 2: Illustration of load P vs. load displacement y curve for (a) the modified technique to determine the critical shear strain release rate G_c for LEFM (b) for an elastic plastic body (LEPFM) for the evaluation if R, J and ω_p. Loading and unloading paths are shown as ↑ and ↓ respectively.

4

Furthermore an attempt was made to characterize slow crack growth data of nuclear graphite. Using Eq.s (2) and (3) *VK* data were determined using the load relaxations and constant displacement rate techniques.

3.3. Linear Elastic-Plastic Fracture Mechanics

The assumption that nuclear graphite indeed experiences some irreversible energy dissipation was verified by Sakai et al [30], where they showed that the loading and unloading curves for CN graphite specimens did not coincide, which leads to the hypothesis of LEPFM. Sakai et al used an approach for the determination of LEPFM fracture parameters, where the assumption is that some plastic deformations significantly contribute to Griffiths modified energy balance, where the net change of work input, ΔW, relates to the change of internal elastic energy ΔU_e, the change of internal plastic energy ΔU_p and the change in surface energy ΔU_γ caused by the extension of the crack.

$$\Delta W = \Delta U_e + \Delta U_p + \Delta U_\gamma \tag{5}$$

Their empirical, graphical method for determining the non linear fracture toughness parameters, R (crack resistance), J (the J integral) and ω_p (plastic energy dissipation rate), as a function of advancing crack lengths, was done by means of calculating the areas under the load displacement curve. This technique made use of cyclic loading and unloading where the empirical values for R, J and ω_p are estimated experimentally as the areas between the loading and unloading curves.

According to Sakai the area $\Delta \pi_R$ enclosed by *BAED* on Fig. 2(b) ($\Delta \pi_p$ and $\Delta \pi_J$ combined) represents the total energy consumed by the extension of a crack by area ΔA and if ΔA is to be small, this energy divided by ΔA is equivalent to the crack growth resistance R. ΔA is simply estimated by $\Delta A = \Delta a * d$ as the crack front shape was shown to remain constant for the DTB specimen [10] [14][16][17] [21][23].

$$\frac{\Delta \pi_R}{\Delta A} = \frac{\Delta}{\Delta A}(w - U_e)_c \equiv R \tag{6}$$

By shifting the loading line *ED* of Fig. 2(b) to the left by the increment of plastic deformation $\Delta \pi_p$ (given as *BE'*), then the area $\Delta \pi_R$ can be split into two distinct portions, $\Delta \pi_p$ and $\Delta \pi_J$. Where $\Delta \pi_p$, enclosed by *BE'ED*, represents the energy absorbed due to the formation of the plastic zone or for graphite the wake region. Similarly, according to Sakai et al, the area $\Delta \pi J$, enclosed by *BAE'*, represents *J*, as *J* is defined as the plastic elastic difference between the linear and nonlinear elastic bodies with the same geometric variables except for the unity differences in crack area [5].

$$\frac{\Delta \pi_J}{\Delta A} = \frac{\Delta}{\Delta A}(w - U_e - U_p)_c \equiv J \tag{7}$$

Similarly, we may define the energy dissipated due to plastic deformation by

$$\frac{\Delta \pi_p}{\Delta A} = \frac{\Delta U_p}{\Delta A} \equiv \omega_p \tag{8}$$

Additionally, it is worth noting that the ψ_{wof}, which is defined as the mean external work which is consumed to produce a unit of fracture surface area during quasi static failure by

5

$$2\psi_{wof} = \frac{\int_0^S R(A)dA}{S} \qquad\qquad (9)$$

and provides useful nonlinear energy fracture toughness parameters, where S is the total fracture area. It has been widely used to characterise the crack growth resistance for complicated non-linear fractures such as those of refractory composites [31][32].

4. Results and Discussion

An example of a load-displacement curve obtained through application of loading and unloading of the DTB of the current graphite material is shown in Fig. 3.

Crack length measurements were undertaken using a microscope mounted on a travelling mechanism with an accuracy of *0.2mm*. There is noticeable crack jumping behaviour (Fig. 3), where the unstable crack growth is represented as a sudden load drop. These load drops were found to be up to *9* percent and are believed to account for large scatter in further *VK* results.
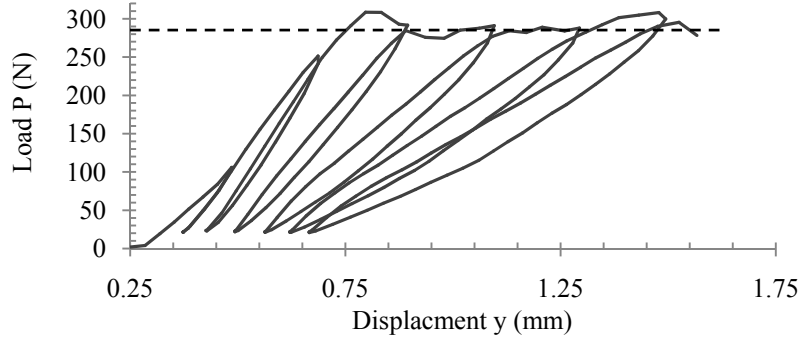

Fig. 3: A standard load displacement curve in stroke control at a ramp rate of 4mm/min. Hysteresis and the offset in the load and unloading curve may be associated with the irreversible energy dissipation process.

4.1. Compliance Relationship

The compliance relationship was found according to Eq. (1), where $C = 3.59 * 10^{-5}(a) + 1.35 * 10^{-3}(mm/N)$ and the theoretical and the experimental compliance were in reasonable agreement.

4.2. Linear Elastic Fracture Mechanics

The fracture toughness of the graphite was calculated according to Eq.4. The critical strain release rate energy G_{Ic} was found and is given in Table 1.

The load relaxation technique in conjunction with the constant displacement technique was used to determine *VK* characteristics. However, the crack jumping behaviour, which is seen as unstable crack propagation, resulted in poor *VK* data. Due to the coarse grain lattice of the graphite there were voids present and it is believed that during relaxation the crack proceeded to propagate steadily until the crack encountered a void in the grain lattice which blunted the crack tip and resulted in a sudden stop. Fig.4(a) of the load relaxation curve is shown to demonstrate this.

Despite this material shortcoming, an attempt was made to solve for the *VK* data from the short relaxation period. The results are shown in Fig. 4 (b) for crack propagation perpendicular and parallel to the preferred grain direction.

The constant displacement rate technique indicated that the load relaxation is flawed as the data points do not coincide. However the constant displacement rate technique also proved inadequate for similar reasons.
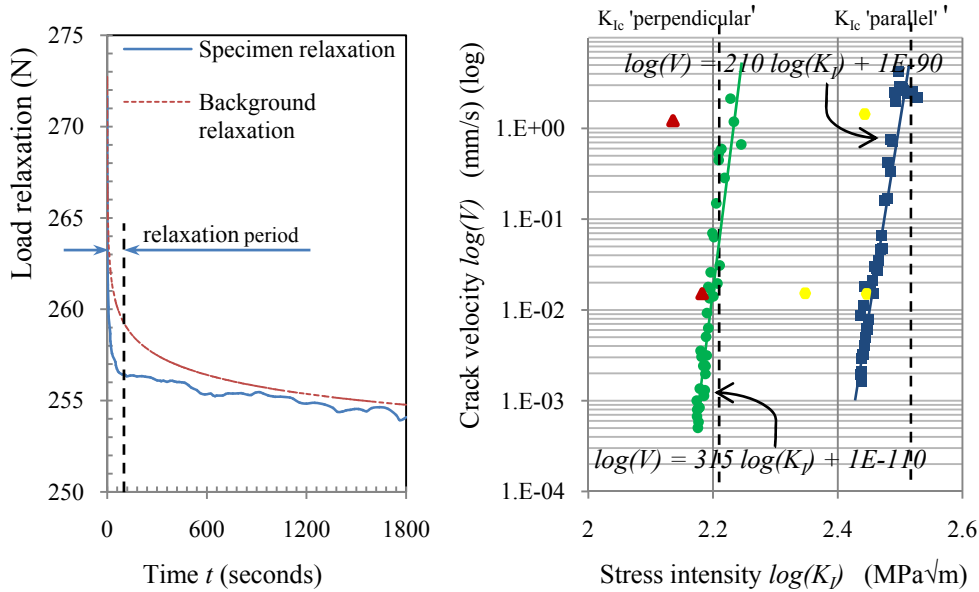

Fig. 4: (a) Relaxation curve of determining vK data showing the specimen and the background relaxation. Notice the quick arrest of the crack tip (<60seconds) resulting in a very short relaxation period. (b)VK data (loglog scale) in the parallel and perpendicular direction. ● perpendicular (load relaxation), ▲ perpendicular (constant displacement rate), ■ parallel (load relaxation), ● parallel(constant displacement rate).

It may be concluded that the difference in K_{Ic} indicate that a higher crack resistance exists in the parallel direction. However, in addition, the slow crack growth data indicated that crack growth in the perpendicular direction is less stable, hinting at comparably denser wake region, containing more micro cracking. The methodology of the DTB, and generation of reliable *VK* data was proven to be acceptable however, only in fine grain or continuous materials. For Perspex (PMMA) excellent and consistent *VK* data were produced using this methodology by Becker [33].

4.3. Linear Elastic-Plastic Fracture Mechanics

The rising *R*-curve behaviour was measured at various notch lengths of *20, 40* and *60mm* (Fig. 5(a)).

It is believed that because the DTB specimen has a constant load plateau, *R*-curves at various crack lengths may be plotted on the same crack extension scale. The results are shown in Fig. 5(b).

Large variance on crack extensions was noticed (up to *50%*) together with a large range in *R* readings *(±20%)*. This is attributed to the crack jumping behaviour, where for large crack extensions significantly less scatter is obtained. For this reason only, tests with larger crack extension were undertaken.
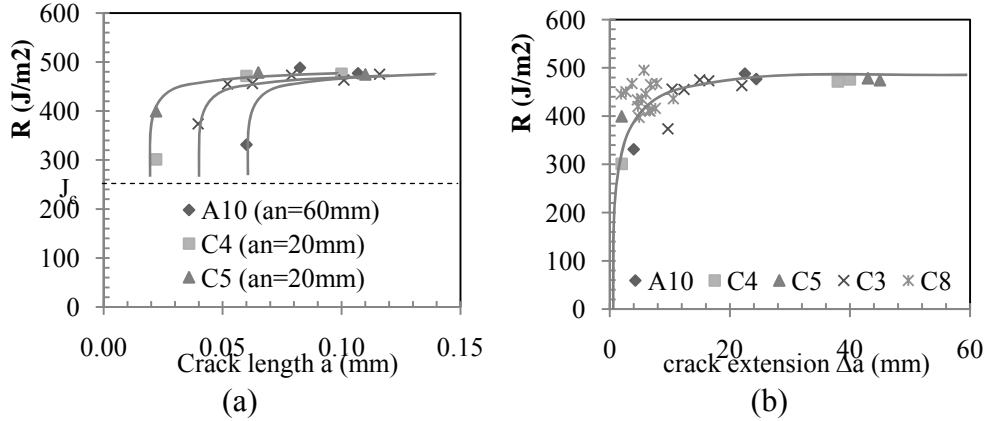

Fig. 5: (a) Typical R-curve behaviour determined by various crack extension. Shown are the results for perpendicular crack propagation. (b) Combined R-curve behaviour of perpendicular specimens at various crack extensions.
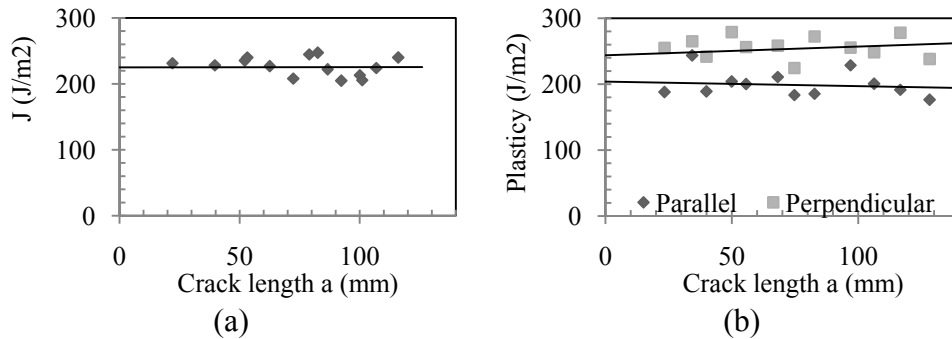

Fig. 6: (a) Plot of J vs. crack length. Test conducted at 4mm/min, (b)Plasticity vs. crack length of perpendicular and parallel specimens at various crack lengths. Both were non pre-crack specimens.

The *J* value was found to reach a plateau value (Fig. 6(a)), which was expected due to the characteristics of the DTB technique having a constant load plateau. If a sufficiently fast crack speed was used *(*displacement rate of *>4mm/min*), neglecting any kinetic and thermal effects, then *J* represents J_c. Results for J_c are given in Table 1. There was no significant difference for the parallel and the perpendicular direction indicating that J_c is the measure of fracture resistance of the graphite material itself, excluding non linear "plasticity" affects.

The plot of plastic energy vs. crack length (Fig. 6(b)) shows the same plateau region indicating that the wake zone remains constant once established. Comparing the plateau area of the specimens which were cracked in the parallel and the perpendicular direction, we may also conclude that the specimens in the perpendicular direction experience larger plasticity effects (by 8%), explained by

8

either a larger or denser process zone, or both. Similar characteristics were also observed in the *R*-curve behaviour for the perpendicular and the parallel cases. Photographic evidence would be needed to make further conclusions on the wake affect.

	Calculated energy (J/m^2)		Equivalent K_{Ic} assuming $J=K^2/E'$ ($MPa\sqrt{m}$)	
	Parallel	Perpendicular	Parallel	Perpendicular
G_{Ic} (LEFM)	*450±40*	*480±55*	*2.2±0.2*	*2.5±0.2*
R (plateau value)	*460±40*	*490±50*	-	-
J_c (plateau value)	*225±30*	*230±30*	*1.3±0.1*	*1.3±0.1*
ω_p (plateau value)	*200±50*	*250±50*	-	-
γ_{wof}	*450*	*480*	-	-

Table 1: Summary of recorded plateau values of the DTB technique. Note: good correlations between γ_{wof} and R were achieved.

5.   Discussion and Concluding Remarks
This DTB technique was successfully employed for the study of fracture toughness and slow crack growth characterisation of nuclear graphite. The technique was adapted for LEPFM for the measure of fracture characteristics of highly brittle materials which experience so called non linear "plasticity" due to micro cracking. The results of slow crack growth investigations are compromised due to the large grain size effect, but it is believed that the technique may be modified for the measure of crack growth in brittle materials which exhibit non linearity.
The tests conducted in this work exhibit extensive micro cracking and crack bridging can contribute up *50%* in coarse grained NVG10 graphite, which is in agreement with Sakai's paper [5], where the elastic-plastic ratio was defined at *0.62* for fine grained graphite. There is some concern about the *J* values determined, as the plane strain criterion was not satisfied and the derivation of the *J* integral assumes plain strain conditions. Although relatively large scatter was encountered, it is believed that the DTB technique can be used for reliable results in nuclear graphite. It is also believed that finer grained graphite can produce better results for VK studies and that slow crack growth data at slower speeds is attainable.
Crack growth resistance curves for the non-linear fracture parameter *R* as a function of crack length were measured in the parallel and perpendicular direction. All of the curves show rising *R*-curve behaviour followed by a plateau region where *R* seems independent of crack length. The initial rising part of the curves was attributed to the development of crack bridges in the wake of the crack front, while in the plateau region the crack bridging zone and the frontal process zone ahead of the crack tip reached steady state values.
The technique proves useful due to its ability to generate stable crack growth over the middle range at constant driving force. It is recommended that further research be conducted on nuclear graphite using the DTB technique as it is believed that this can contribute to the fracture and slow crack growth characterisation of nuclear graphite.

References

[1] The Pebble Bed Modular Reactor project, [Online], Available: www.pbmr.com. [Accessed: Oct. 17, 2008].

[2] B.T. Kelly, Applied Science Publishers, London, 1981

[3] C.A. Anderson, E.I. Salkovitz, ed. R.C. Bradt, D.P.H. Hassleman, F.F. Lange, Plenum, New York, pp.509-526, 1974.

[4] G.R. Romanoski, ed. T.D. Burchel, Oxford Pergamum, pp.484-534, 1999.

[5] M. Sakai, K. Urashima, and M. Inagaki, J. Am. Ceram. Soc., vol.66, pp.868-874, 1983.

[6] W.N. Reynolds, Am. Elsevier Pub. Co., New York, 1968

[7] L. Shi, H. Li, Z. Zou, A.S.L. Fok, B.J. Marsden, A. Hodgkins, P.M. Mummery, J. Marrow, J. Nucl. Mater., vol.372, pp.141–151, 2008

[8] O. J. Outwater and D. J. Gerry. Journal of Adhesion, pp.290, 1966.

[9] A.J. Kies, B.J. Clark, Chapman & Hall, London, pp.483, 1969.

[10] A. G. Evans, J. Mat. Sci., vol.1, p165, 1974.

[11] D. P. Williams, A. G. Evans, J. of Testing Evaluation, vol.1, p.264, 1973.

[12] J. O. Outwater, M. C. Murphy, R. G. Kumble. J. Mater. Sci., pp.127–138, 1974.

[13] H. R. McKinney, H. L. Smith, Am. Ceram. Soc. Bulletin, pp.784, 1971.

[14] A.V. Virkar, R.S. Gordon, J. Am. Ceram. Soc., vol.58, pp.536–536, 1975.

[15] G.G. Trentina, J. Am. Ceram. Soc., vol.60 pp.338–341, 1977.

[16] E.R. Fuller, Am. Soc. for Test. Mater., p.3, 1979.

[17] B.J. Pletka, E.R. Fuller, B.G. Koepke, Am. Soci. Test. Mater., p.19, 1979.

[18] R. B. Tait, P. Fry, G.G. Garret, vol.27, pp.14-22, 1987.

[19] A. Shyam, E. Lara-Curzio, J. Mat. Sci., vol.41 pp.4093– 4104, 2006.

[20] P.S. Leevers, J. Mat. Sci., vol.17 pp.2468–2480, 1982.

[21] P.S. Leevers, J. Mat. Sci., vol.20 pp.77–84, 1985.

[22] P.S. Leevers, J. Mat. Sci. Letters, vol.5 pp.191–192, 1986.

[23] J. Chevalier, M. Saadaoui, C. Olagnon, G. Fantozzi, J. C. Int., vol.22 pp.171–177, 1996.

[24] M. Ciccotti, PhD Thesis, Universita di Bologna, 1999.

[25] M. Ciccotti, J. Am. Ceram. Soc., vol.83 pp.2737–2744, 2000.

[26] M. Ciccotti, G. Gonzato, F. Mulargia, Int. J. Rock Mech. Mining Sci., vol.37 pp.1103–1113, 2000.

[27] M. Ciccotti, N. Nigri ,G. Gonzato, F. Mulargia,. Int. J. Rock Mech. Mining Sci., vol.38 pp.569–576, 2001.

[28] J. C. Pollet S. J. Burns, J. Am. Ceram. Soc. Discussion and Notes, vol.62 pp.426–427, 1979.

[29] M.C.F. Albuquerqu, J.A. Rodrigues, Mater. Research, vol. 9, pp.361-368, 2006

[30] M. Sakai, J. Yoshimura, Y. Goto, M. Inagak, Am. Ceram. Soc., vol.71, pp.608-616, 1988.

[31] Nakayama, J. Am. Ceram. Soc., vol.48. pp.583-87, 1965

[32] J. Homeny, T. Darroudi, R.C. Bradt, J. Am. Ceram. Soc. vol.48, pp.326-331, 1980

[33] T. Becker, MSc Thesis, University of Cape Town, 2008 (not published)